Light scattering from slightly rough semiconductor surfaces near exciton resonance

J. Madrigal-Melchor
Escuela de Física, Universidad Autónoma de Zacatecas, Apartado Postal C-580, Zacatecas, Zacatecas 98060, Mexico

H. Azucena-Coyotécatl
Escuela de Ciencias de la Electrónica, Universidad Autónoma de Puebla, C. U., Puebla, Puebla 72570, Mexico

A. Silva-Castillo and F. Pérez-Rodríguez
Instituto de Física, Universidad Autónoma de Puebla, Apartado Postal J-48, Puebla, Puebla 72570, Mexico
(Received 8 December 1999)

The phenomenon of light scattering by a randomly rough surface and fluctuations of the excitonic surface potential is investigated by means of a first-order perturbation theory. We employ the generalized Morse potential to describe both intrinsic (repulsive) potentials and extrinsic near-surface potential wells. Frequency and angle dependencies of the light-scattering cross section are calculated. A considerable increase of the scattering cross section, as the correlation between the surface roughness and the excitonic potential fluctuations diminishes, is observed. Our theory describes very well available experimental results for samples with a repulsive surface potential. Also, the optical manifestation of excitonic bound states, generated within a surface-potential well, is analyzed. We find that the near-surface localized excitons produce a resonance structure in the spectrum of the light-scattering cross section, which is very sensitive to the degree of correlation between surface roughness and potential-well fluctuations.

I. INTRODUCTION

For a long time the phenomenon of light scattering from rough surfaces had been a topic of great interest to researchers (see, for example, Refs. 1–17). This phenomenon is notably affected not only by the characteristics of the surface profile of the irradiated medium, but also by its bulk optical properties such as spatial dispersion or nonlocality.[18] This property of the medium leads to a wave-vector dependence of the dielectric function and to the generation of additional electromagnetic modes that influence upon a variety of optical spectra. In particular, spatial dispersion has a significant effect on light scattering from rough surfaces of metallic[3–7] and excitonic[3,4,8–16] media.

In the case of excitonic crystals, besides nonlocal effects, the interaction of the exciton with the sample surface plays a fundamental role.[19] In a simple approach, this interaction can be taken into account by choosing appropriate additional boundary conditions[19] (ABC) needed to determine the amplitudes of the generated modes, since the usual Maxwell boundary conditions (continuity of the tangential electric and magnetic fields at the sample surface) are not sufficient. Within this approach the spectra of light scattering turn out to be fairly sensitive to the choice of the ABC as is shown in Refs. 8 and 9.

The interaction of excitons with the sample surface can also be described by using a surface potential.[19] In crystals of relatively high quality the surface potential is given by intrinsic contributions, which are determined, principally, by the no-escape condition for the electron and hole[20,21] and the image potential.[20,22] As a result, the intrinsic potential repels excitons from the near-surface region.[20] The simplest model for such a potential consists of an infinite barrier at certain distance from the surface, of the order of the exciton radius. This barrier produces a near-surface layer, where excitons are absent (exciton-free layer or dead layer[22]). For many years, this model was widely applied for interpreting reflectivity measurements. However, the dead-layer model has various problems:[19,23] (i) appropriate ABC at the fictitious interface have to be specified, (ii) it cannot describe the reflectivity distortion associated with the finite slope of the real (continuous) surface potential for the translational exciton motion, and (iii) the fits based on this model are not sufficiently accurate for III-V semiconductors, having relatively small longitudinal-transverse splitting. In a set of papers[10–15] the dead-layer model was also used to analyze light scattering from rough surfaces. There it was shown that surface roughness gives rise to fluctuations of the inner boundary of the dead layer, which affect considerably spectra of the light-scattering cross section.

A trustworthy description of the surface-potential shape requires the use of a model more sophisticated than the dead layer, especially when the potential has an extrinsic contribution, which can be caused either unintentionally during the process of crystal growth or by surface treatments. Indeed, electron[24–26] and ion[27–29] bombardment, intense illumination,[30–33] heating,[34] and the application of an electric field[32,33,35] give rise to a near-surface space-charge region and, consequently, a macroscopic electric field with which excitons interact.[32,36,37] Due to this interaction, an attractive part in the surface potential can appear, and thus a potential well may be formed. The generation of exciton bound states within near-surface potential wells and their manifestation in optical spectra for samples with ideal flat surfaces have been widely analyzed (see, for instance Refs. 19, 25, and 36–40). Today it is well established that reflectivity spectra exhibit broad peaks (transverse resonances[39,41–43]) at frequencies ω_{Tn} close to the eigenvalues of excitonic bound states. More-

over, the coupling of the localized excitons with the electromagnetic field inside the semiconductor depends strongly on the polarization of the incident light.[24,40,44] As a result, the resonance structures of reflectivity spectra for *s*-polarized light and *p*-polarized light turn out to be very different. In the *p*-polarization geometry, additional resonances (dips) appear in the reflectivity spectra. The new resonances are associated with quantized polarization waves (longitudinal modes), whose eigenfrequencies ω_{Ln} are shifted with respect to the frequencies ω_{Tn} of transverse resonances as $\omega_{Ln}=\omega_{Tn}+\omega_{LT}$ (Refs. 40 and 44) (ω_{LT} is the frequency value of the longitudinal-transverse splitting). The longitudinal modes are well identified by employing 45° reflectometry.[45]

Recently,[46] the manifestation of near-surface localized excitons in spectra of light scattering from rough surfaces was investigated theoretically by us. In that work, a model for the surface potential that takes into account its random fluctuations produced by the surface roughness, was employed. By assuming a complete correlation between potential-well fluctuations and surface roughness, it was shown in Ref. 46 that a resonance structure in the spectrum of light-scattering cross section appears because of the generation of exciton bound states. The assumption of complete correlation between potential fluctuations and the surface profile is an important limitation of our previous theory,[46] since the presence of impurities or defects in the near-surface layer (especially in an extrinsic transition layer) can diminish such a correlation,[13,14] and therefore both frequency and angle dependencies of the light-scattering cross section may be altered.

The aim of the present work is to investigate theoretically the light scattering from slightly rough semiconductor surfaces near exciton resonance, particularly when the surface roughness and the excitonic potential fluctuations are not completely correlated. In Sec. II we present in detail the theoretical formalism applied to calculate the light-scattering cross section for a semi-infinite excitonic medium. In Secs. III and IV, we study the effect of the degree of correlation between potential fluctuations and surface roughness on light-scattering spectra in the cases of intrinsic and extrinsic transition layers, respectively. We compare our theoretical spectra with available experimental results for samples of relatively high quality (Sec. III). The spectra of light-scattering cross sections in the presence of near-surface localized excitons are analyzed in Sec. IV.

II. THEORY

A. Formulation of the problem

Let us consider a system consisting of a semiconductor in the region $z>\zeta_r(\mathbf{r}_\parallel)$, where $\mathbf{r}_\parallel=(x,y,0)$, and of vacuum in the region $z<\zeta_r(\mathbf{r}_\parallel)$. Here, the function $\zeta_r(\mathbf{r}_\parallel)$ describes the profile of the semiconductor surface, which is assumed to be slightly rough and random with small slopes $[|\nabla\zeta_r(\mathbf{r}_\parallel)|\ll 1]$ and a small characteristic deviation δ_r from the average surface $z=0$. The function $\zeta_r(\mathbf{r}_\parallel)$ of the surface profile is a zero-mean, stationary, Gaussian random process, determined by the properties

$$\langle\zeta_r(\mathbf{r}_\parallel)\rangle=0,\quad \langle\zeta_r(\mathbf{r}_\parallel)\zeta_r(\mathbf{r}'_\parallel)\rangle=\delta_r^2\exp[|\mathbf{r}_\parallel-\mathbf{r}'_\parallel|^2/L_r^2]. \quad (1)$$

Here, the angle brackets denote an average over the ensemble of realizations of the function $\zeta_r(\mathbf{r}_\parallel)$ and L_r is the correlation length ($L_r\gg\delta_r$).

The incident field has the form

$$\mathbf{E}_i(\mathbf{r},t)=E_i[\cos\sigma(\hat{\mathbf{x}}\cos\theta_i-\hat{\mathbf{z}}\sin\theta_i)+\hat{\mathbf{y}}\sin\sigma]\times e^{i(k_x x+k_z z)-i\omega t}, \quad (2)$$

where $k_x=k\sin\theta_i$ ($\mathbf{k}_\parallel=k_x\hat{\mathbf{x}}$), $k_z=k\cos\theta_i$, $k=\omega/c$, ω is the frequency, c is the velocity of light in vacuum, and θ_i and σ are the angles of incidence (in the xz plane) and polarization, respectively. If $\sigma=0$ ($\pi/2$) the incident wave is p (s) polarized. Applying perturbation theory up to first order in $k\delta_r\ll 1$ and $|\nabla\zeta_r(\mathbf{r}_\parallel)|\ll 1$, the scattered field can be expressed as

$$\mathbf{E}_{sc}=\mathbf{E}_{sc}^{(0)}+\mathbf{E}_{sc}^{(1)}, \quad (3)$$

where the zeroth-order field

$$\mathbf{E}_{sc}^{(0)}(\mathbf{r},t)=[E_p^{(0)}(k_x)(\hat{\mathbf{x}}\cos\theta_i+\hat{\mathbf{z}}\sin\theta_i)+E_s^{(0)}(k_x)\hat{\mathbf{y}}]e^{i(k_x x-k_z z)-i\omega t}, \quad (4)$$

and the first-order field is given by

$$\mathbf{E}_{sc}^{(1)}(\mathbf{r},t)=\int\frac{d^2k'_\parallel}{(2\pi)^2}\mathbf{E}_{sc}^{(1)}(\mathbf{k}'_\parallel)e^{i(\mathbf{k}'_\parallel\cdot\mathbf{r}_\parallel-k'_z z)-i\omega t}, \quad (5)$$

$$\mathbf{E}_{sc}^{(1)}(\mathbf{k}'_\parallel)=\hat{\mathbf{T}}[E_p^{(1)}(\mathbf{k}'_\parallel)(\hat{\mathbf{x}}'\cos\theta'+\hat{\mathbf{z}}'\sin\theta')+E_s^{(1)}(\mathbf{k}'_\parallel)\hat{\mathbf{y}}'], \quad (6)$$

where $\hat{\mathbf{x}}'=\mathbf{k}'_\parallel/k'_\parallel$ ($k'_\parallel=|k'_{x'}|$), $\hat{\mathbf{z}}'=\hat{\mathbf{z}}$, and $\hat{\mathbf{y}}'=\hat{\mathbf{z}}'\times\hat{\mathbf{x}}'$; $\hat{\mathbf{T}}$ is a rotation matrix with nonzero elements $T_{xx'}=T_{yy'}=k'_x/k'_\parallel$, $T_{xy'}=-T_{yx'}=-k'_y/k'_\parallel$, and $T_{zz'}=1$; θ' is the angle of scattering in the $x'z'$ plane, $k'_{x'}=k\sin\theta'$, and $k'_{z'}=(k^2-(k'_{x'})^2)^{1/2}=k\cos\theta'$.

Inside the semiconductor, the electric field $\mathbf{E}$ and the excitonic polarization $\mathbf{P}$ are described by a system of coupled equations:[19]

$$\nabla^2\mathbf{E}-\nabla(\nabla\cdot\mathbf{E})+\epsilon_\infty k^2\mathbf{E}=-4\pi k^2\mathbf{P}, \quad (7)$$

$$\left[-\frac{\hbar\omega_T}{M}\nabla^2+\omega_T^2-\omega^2-i\nu\omega+\frac{2\omega_T U(\mathbf{r}_\parallel,z)}{\hbar}\right]\mathbf{P}=\frac{\omega_P^2}{4\pi}\mathbf{E}, \quad (8)$$

where ϵ_∞ is the high-frequency (background) dielectric constant, M is the translational exciton mass, ω_T is the exciton resonance frequency, ω_P is a measure of the oscillator strength, and the damping constant ν describes the lifetime broadening. The wave equation (7) for $\mathbf{E}$ is obtained from Maxwell equations, and Eq. (8) for $\mathbf{P}$ is derived from the exciton motion within the adiabatic approximation.[19]

Due to the surface roughness, the surface potential U in Eq. (8) depends not only on the coordinate z, but also on $\mathbf{r}_\parallel$. If the semiconductor surface is sufficiently smooth such that $L_r\gg a$ (a is the characteristic size of the surface transition layer), the exciton interacts *locally* with a flat region of the smooth surface. In this case, the surface potential depends parametrically on $\mathbf{r}_\parallel$ and is given by $U(\mathbf{r}_\parallel,z)=U(z-\zeta_r(\mathbf{r}_\parallel))$, where $U(z)$ is the potential for an ideal flat sur-

face. Assuming a very small roughness ($\delta_r \ll a$), we can approximate the surface potential $U(\mathbf{r}_\parallel, z)$ up to linear terms in ζ_r:

$$U(\mathbf{r}_\parallel, z) \approx U(z) - \frac{dU(z)}{dz}\zeta_r(\mathbf{r}_\parallel), \quad \delta_r \ll a \ll L_r. \tag{9}$$

Let us emphasize that Eq. (9) is valid when there is a complete correlation between the fluctuations of the surface potential and the profile of the rough surface. As was mentioned in the Introduction, the presence of impurities or defects in the transition layer can substantially diminish such a correlation. In describing the latter situation, we shall assume here that the potential fluctuations, produced by the two kinds of disorder (surface roughness and near-surface defects), are sufficiently small to be treated as a perturbation. Hence, we can use an expansion of the real surface potential $U(\mathbf{r}_\parallel, z)$ similar to Eq. (9),

$$U(\mathbf{r}_\parallel, z) = U(z) - \frac{dU(z)}{dz}\zeta_f(\mathbf{r}_\parallel), \quad \delta_f \ll a \ll \min\{L_f, L_r, L_{rf}\}, \tag{10}$$

where the function $\zeta_f(\mathbf{r}_\parallel)$ is also a zero-mean, Gaussian random process, characterized by the following statistical properties:

$$\langle \zeta_f(\mathbf{r}_\parallel)\rangle = 0, \ \langle \zeta_f(\mathbf{r}_\parallel)\zeta_f(\mathbf{r}'_\parallel)\rangle = \delta_f^2 \exp[|\mathbf{r}_\parallel - \mathbf{r}'_\parallel|^2/L_f^2] \tag{11}$$

and

$$\langle \zeta_r(\mathbf{r}_\parallel)\zeta_f(\mathbf{r}'_\parallel)\rangle = \delta_r \delta_f \kappa_{rf} \exp[|\mathbf{r}_\parallel - \mathbf{r}'_\parallel|^2/L_{rf}^2]. \tag{12}$$

Here δ_f and L_f are the average value and the correlation length of $\zeta_f(\mathbf{r}_\parallel)$, respectively; L_{rf} is the mutual correlation length for functions $\zeta_r(\mathbf{r}_\parallel)$ and $\zeta_f(\mathbf{r}_\parallel)$, and $\kappa_{rf} = \langle \zeta_r(0)\zeta_f(0)\rangle/(\delta_r\delta_f)$ is a correlation coefficient satisfying the condition $|\kappa_{rf}| \leqslant L_r L_f/L_{rf}^2 \leqslant 2L_rL_f/(L_r^2+L_f^2) \leqslant 1$.[14,17] In our model (10) the random part of the potential $U(\mathbf{r}_\parallel, z)$ depends statistically only on $\mathbf{r}_\parallel$, whereas its z dependence is deterministic. As we will see below, although the chosen model (10) for the potential $U(\mathbf{r}_\parallel, z)$ is quite simple, it turns out to be good enough to interpret and reproduce experimental spectra of light scattering not only in the case of high correlation between the potential fluctuations and the profile of the semiconductor surface [$\zeta_f(\mathbf{r}_\parallel) \approx \zeta_r(\mathbf{r}_\parallel)$], but also when such a correlation is low.

Considering that the excitonic potential $U(z)$ for an ideal flat surface is well modeled by the generalized Morse potential,[39,40] the surface potential $U(\mathbf{r}_\parallel, z)$ (10) can be expressed as

$$U(\mathbf{r}_\parallel, z) = U_1 e^{-z/a} + U_2 e^{-2z/a} + \zeta_f(\mathbf{r}_\parallel) \times (U_1 e^{-z/a} + 2U_2 e^{-2z/a})/a. \tag{13}$$

This form of the surface potential allows to solve analytically the system of Eqs. (7) and (8). Indeed, let us write the exciton-polariton fields $\mathbf{E}$ and $\mathbf{P}$ in terms of only zeroth- and first-order contributions in $k\delta_r \ll 1$, $|\nabla \zeta_r| \ll 1$, $\delta_r/a \ll 1$, and $\delta_f/a \ll 1$:

$$\mathbf{E} = \mathbf{E}^{(0)} + \mathbf{E}^{(1)}, \quad \mathbf{P} = \mathbf{P}^{(0)} + \mathbf{P}^{(1)}. \tag{14}$$

Using Eqs. (13) and (14), we can rewrite the system of Eqs. (7) and (8) in the form

$$4\pi k^2 \mathbf{P}^{(0)} + \nabla^2 \mathbf{E}^{(0)} - \nabla(\nabla \cdot \mathbf{E}^{(0)}) + \epsilon_\infty k^2 \mathbf{E}^{(0)} = 0, \tag{15}$$

$$\left[-\frac{\hbar\omega_T}{M}\nabla^2 + \omega_T^2 - \omega^2 - i\nu\omega + \frac{2\omega_T}{\hbar}(U_1 e^{-z/a} + U_2 e^{-2z/a}) \right] \mathbf{P}^{(0)} - \frac{\omega_P^2}{4\pi}\mathbf{E}^{(0)} = 0, \tag{16}$$

$$4\pi k^2 \mathbf{P}^{(1)} + \nabla^2 \mathbf{E}^{(1)} - \nabla(\nabla \cdot \mathbf{E}^{(1)}) + \epsilon_\infty k^2 \mathbf{E}^{(1)} = 0, \tag{17}$$

$$\left[-\frac{\hbar\omega_T}{M}\nabla^2 + \omega_T^2 - \omega^2 - i\nu\omega + \frac{2\omega_T}{\hbar}(U_1 e^{-z/a} + U_2 e^{-2z/a}) \right] \mathbf{P}^{(1)} - \frac{\omega_P^2}{4\pi}\mathbf{E}^{(1)} = -\frac{2\omega_T}{\hbar}\frac{\zeta_f(\mathbf{r}_\parallel)}{a}(U_1 e^{-z/a} + 2U_2 e^{-2z/a})\mathbf{P}^{(0)}, \tag{18}$$

The solutions of Eqs. (15) and (16) describe the exciton-polariton fields in the absence of both potential fluctuations and surface roughness and have been analytically calculated in Refs. 39 and 40. Since those solutions are necessary to obtain the first-order polaritonic fields [$\mathbf{P}^{(1)}$ and $\mathbf{E}^{(1)}$ in Eqs. (17) and (18)], below we shall present them in a compact form.

B. Zeroth-order solutions

According to the assumed geometry of the problem, we can rewrite the system of Eqs. (15) and (16) in terms of only $\mathbf{P}^{(0)}$ components as follows:

$$\frac{\partial^4 P_y^{(0)}}{\partial z^4} + [\beta + \Delta]\frac{\partial^2 P_y^{(0)}}{\partial z^2} + 2\frac{\partial \Delta}{\partial z}\frac{\partial P_y^{(0)}}{\partial z} + \left[\beta\Delta + \frac{\partial^2 \Delta}{\partial z^2} - \alpha k^2 \right] P_y^{(0)} = 0, \tag{19}$$

$$ik_x \left[\frac{\partial^3 P_x^{(0)}}{\partial z^3} + \Delta\frac{\partial P_x^{(0)}}{\partial z} + \frac{\partial \Delta}{\partial z}P_x^{(0)} \right] - \beta\frac{\partial^2 P_z^{(0)}}{\partial z^2} + [\alpha k^2 - \beta\Delta]P_z^{(0)} = 0, \tag{20}$$

$$\frac{\partial^4 P_x^{(0)}}{\partial z^4} + [\beta + \Delta]\frac{\partial^2 P_x^{(0)}}{\partial z^2} + 2\frac{\partial \Delta}{\partial z}\frac{\partial P_x^{(0)}}{\partial z} + \left[\beta\Delta + \frac{\partial^2 \Delta}{\partial z^2} - \frac{\alpha k^2 \beta}{k_x^2 + \beta} \right] P_x^{(0)} - \frac{ik_x \alpha k^2}{k_x^2 + \beta}\frac{\partial P_z^{(0)}}{\partial z} = 0, \tag{21}$$

where

$$\alpha = \frac{\omega_P^2 M}{\hbar\omega_T}, \quad \beta = \epsilon_\infty k^2 - k_x^2, \tag{22}$$

$$\Delta(z)=\frac{M}{\hbar\omega_T}\left[\omega^2-\omega_T^2+i\omega\nu-\frac{2\omega_T}{\hbar}(U_1e^{-z/a}+U_2e^{-2z/a})\right]-k_x^2. \tag{23}$$

In obtaining Eqs. (19), (20), and (21) we have taken into account that the zeroth-order fields are proportional to $\exp(ik_x x)$. The solutions of these equations can be written as [39,40]

$$P_y^{(0)}(z)=\sum_{m=1}^{2}A_m^{(0)}e^{ik_m z}\sum_{n=0}^{\infty}a_{y,nm}e^{-nz/a}, \tag{24}$$

$$P_j^{(0)}(z)=\sum_{m=1}^{3}B_m^{(0)}e^{ik_m z}\sum_{n=0}^{\infty}a_{j,nm}e^{-nz/a},\quad j=x,z. \tag{25}$$

Here k_m $(m=1,2,3,\ \mathrm{Im}\,k_m>0)$ is the z component of the wave vectors for polaritonic modes that propagate in the bulk where the surface potential is negligible $[U(z)\to 0]$. The quantities k_1 and k_2 correspond to transverse modes and are given by

$$k_{1,2}=\left\{\frac{1}{2}\left[\frac{M}{\hbar\omega_T}[\omega^2-\omega_T^2+i\omega\nu]-k_x^2+\beta \pm\left[\left(\frac{M}{\hbar\omega_T}[\omega^2-\omega_T^2+i\omega\nu]-k_x^2-\beta\right)^2+4\alpha\xi\right]^{1/2}\right]\right\}. \tag{26}$$

The mode $m=3$ in Eq. (25) is a longitudinal one, for which

$$k_3=\left(\frac{M}{\hbar\omega_T}[\omega^2-\omega_T^2+i\omega\nu]-k_x^2-\frac{\omega_P^2 M}{\epsilon_\infty\hbar\omega_T}\right)^{1/2}. \tag{27}$$

The coefficients $a_{j,nm}$ $(j=x,y,z)$ in series (24) and (25) are found from recursion relations, which are straightforwardly obtained by substituting these series into Eqs. (19), (20), and (21). We will not present here the recursion relations for $a_{j,nm}$ because of their cumbersome form. Finally, $A_m^{(0)}$ and $B_m^{(0)}$ in Eqs. (24) and (25) are the amplitudes of the zeroth-order fields to be calculated by using boundary conditions. The expression for the electric field $\mathbf{E}^{(0)}$ is easily derived from Eqs. (16), (24), and (25).

C. First-order solutions

In order to solve the system of Eqs. (17) and (18) it is convenient to express the first-order fields as

$$\mathbf{E}^{(1)}(\mathbf{r})=\int\frac{d^2k_\parallel'}{(2\pi)^2}\hat{\mathbf{T}}[E_{x'}^{(1)}(\mathbf{k}_\parallel',z)\hat{\boldsymbol{x}}'+E_{y'}^{(1)}(\mathbf{k}_\parallel',z)\hat{\boldsymbol{y}}'+E_z^{(1)}(\mathbf{k}_\parallel',z)\hat{\mathbf{z}}]e^{i\mathbf{k}_\parallel'\cdot\mathbf{r}_\parallel}, \tag{28}$$

$$\mathbf{P}^{(1)}(\mathbf{r})=\int\frac{d^2k_\parallel'}{(2\pi)^2}\hat{\mathbf{T}}[P_{x'}^{(1)}(\mathbf{k}_\parallel',z)\hat{\boldsymbol{x}}'+P_{y'}^{(1)}(\mathbf{k}_\parallel',z)\hat{\boldsymbol{y}}'+P_z^{(1)}(\mathbf{k}_\parallel',z)\hat{\mathbf{z}}]e^{i\mathbf{k}_\parallel'\cdot\mathbf{r}_\parallel}, \tag{29}$$

Using Eqs. (17), (18), (28), and (29), we get a system of equations for the Fourier transforms $\mathbf{E}^{(1)}(\mathbf{k}_\parallel',z)$ and $\mathbf{P}^{(1)}(\mathbf{k}_\parallel',z)$ in the coordinate system $x'y'z$:

$$\left[\frac{\partial^2}{\partial z^2}+\Delta'\right]P_j^{(1)}(\mathbf{k}_\parallel',z)+F_j(\mathbf{k}_\parallel',z)=-\frac{\alpha}{4\pi}E_j^{(1)}(\mathbf{k}_\parallel',z),\quad j=x',y',z \tag{30}$$

$$\left[\frac{\partial^2}{\partial z^2}+\beta'\right]E_{y'}^{(1)}(\mathbf{k}_\parallel',z)=-4\pi k^2P_{y'}^{(1)}(\mathbf{k}_\parallel',z), \tag{31}$$

$$\left[\frac{\partial^2}{\partial z^2}+\epsilon_\infty k^2\right]E_{x'}^{(1)}(\mathbf{k}_\parallel',z)-ik_\parallel'\frac{\partial}{\partial z}E_z^{(1)}(\mathbf{k}_\parallel',z)=-4\pi k^2P_{x'}^{(1)}(\mathbf{k}_\parallel',z), \tag{32}$$

$$ik_\parallel'\frac{\partial}{\partial z}E_{x'}^{(1)}(\mathbf{k}_\parallel',z)-\beta'E_z^{(1)}(\mathbf{k}_\parallel',z)=4\pi k^2P_z^{(1)}(\mathbf{k}_\parallel',z). \tag{33}$$

Here α is defined as in Eq. (22), $\beta'=\epsilon_\infty k^2-(k_\parallel')^2$, and

$$\Delta'(z)=\frac{M}{\hbar\omega_T}\left[\omega^2-\omega_T^2+i\omega\nu-\frac{2\omega_T}{\hbar}(U_1e^{-z/a}+U_2e^{-2z/a})\right]-(k_\parallel')^2. \tag{34}$$

Quantities $F_j(\mathbf{k}_\parallel',z)$ $(j=x',y',z)$ in Eq. (30) are the components of the vector

$$\mathbf{F}(\mathbf{k}_\parallel',z)=-\frac{2M}{\hbar^2a}(U_1e^{-z/a}+2U_2e^{-2z/a})\times\zeta_f(\mathbf{k}_\parallel'-\mathbf{k}_\parallel)\hat{\mathbf{T}}^{-1}\mathbf{P}^{(0)}(z), \tag{35}$$

where $\mathbf{P}^{(0)}(z)$ is the zeroth-order excitonic polarization [see Eqs. (24) and (25)] and $\zeta_f(\mathbf{k}_\parallel')$ is the Fourier transform of $\zeta_f(\mathbf{r}_\parallel)$,

$$\zeta_f(\mathbf{k}_\parallel')=\int d^2r_\parallel e^{-i\mathbf{k}_\parallel'\cdot\mathbf{r}_\parallel}\zeta_f(\mathbf{r}_\parallel). \tag{36}$$

After eliminating the electric field from Eqs. (30–33), we get an inhomogeneous system of equations for $P_j^{(1)}(\mathbf{k}_\parallel',z)$ $(j=x',y',z)$ in the form

$$\frac{\partial^4P_{y'}^{(1)}}{\partial z^4}+[\beta'+\Delta']\frac{\partial^2P_{y'}^{(1)}}{\partial z^2}+2\frac{\partial\Delta'}{\partial z}\frac{\partial P_{y'}^{(1)}}{\partial z}+\left[\beta'\Delta'+\frac{\partial^2\Delta'}{\partial z^2}-\alpha k^2\right]P_{y'}^{(1)}+\beta'F_{y'}+\frac{\partial^2F_{y'}}{\partial z^2}=0, \tag{37}$$

$$ik_\parallel'\left[\frac{\partial^3P_{x'}^{(1)}}{\partial z^3}+\Delta'\frac{\partial P_{x'}^{(1)}}{\partial z}+\frac{\partial\Delta'}{\partial z}P_{x'}^{(1)}\right]-\beta'\frac{\partial^2P_z^{(1)}}{\partial z^2}+[\alpha k^2-\beta'\Delta']P_z^{(1)}+ik_\parallel'\frac{\partial F_{x'}}{\partial z}-\beta'F_z=0, \tag{38}$$

$$\frac{\partial^4 P^{(1)}_{x'}}{\partial z^4}+[\beta'+\Delta']\frac{\partial^2 P^{(1)}_{x'}}{\partial z^2}+2\frac{\partial \Delta'}{\partial z}\frac{\partial P^{(1)}_{x'}}{\partial z}+\left[\beta'\Delta'+\frac{\partial^2\Delta'}{\partial z^2}-\frac{\alpha k^2\beta'}{(k'_\parallel)^2+\beta'}\right]P^{(1)}_{x'}-\frac{ik'_\parallel \alpha k^2}{(k'_\parallel)^2+\beta'}\frac{\partial P^{(1)}_z}{\partial z}+\beta' F_{x'}+\frac{\partial^2 F_{x'}}{\partial z^2}=0, \tag{39}$$

The solutions of this system of equations can be written as

$$P^{(1)}_{y'}(\mathbf{k}'_\parallel,z)=a^2\sum_{m=1}^{2}A^{(1)}_m e^{ik'_m z}\sum_{n=0}^{\infty}b_{y',nm}e^{-nz/a}+\frac{\zeta_f(\mathbf{k}'_\parallel-\mathbf{k}_\parallel)}{a}\sum_{m=1}^{2}A^{(0)}_m e^{ik_m z}\sum_{n=0}^{\infty}c_{y',nm}e^{-nz/a}+\frac{\zeta_f(\mathbf{k}'_\parallel-\mathbf{k}_\parallel)}{a}\sum_{m=1}^{3}B^{(0)}_m e^{ik_m z}\sum_{n=0}^{\infty}d_{y',nm}e^{-nz/a}, \tag{40}$$

$$P^{(1)}_{j}(\mathbf{k}'_\parallel,z)=a^2\sum_{m=1}^{3}B^{(1)}_m e^{ik'_m z}\sum_{n=0}^{\infty}b_{j,nm}e^{-nz/a}+\frac{\zeta_f(\mathbf{k}'_\parallel-\mathbf{k}_\parallel)}{a}\sum_{m=1}^{2}A^{(0)}_m e^{ik_m z}\sum_{n=0}^{\infty}c_{j,nm}e^{-nz/a}+\frac{\zeta_f(\mathbf{k}'_\parallel-\mathbf{k}_\parallel)}{a}\sum_{m=1}^{3}B^{(0)}_m e^{ik_m z}\sum_{n=0}^{\infty}d_{j,nm}e^{-nz/a},\quad j=x',z. \tag{41}$$

Here, the first term on the right-hand side of Eqs. (40) and (41) corresponds to the homogeneous solution for the system of Eqs. (37), (38), and (39). The particular solution of this system is given by the terms proportional to $\zeta_f(\mathbf{k}'_\parallel-\mathbf{k}_\parallel)$ in Eqs. (40) and (41). The expressions for the wave-vector components k'_m ($m=1,2,3$, $\mathrm{Im}\,k'_m>0$), appearing in the homogeneous solution, are obtained from the formulas (26) and (27) for k_m by writing there $k'_\parallel$ and β' instead of k_x and β, respectively. The coefficients $b_{j,nm}$, $c_{j,nm}$, and $d_{j,nm}$ ($j=x',y',z$) obey recursion relations, which are straightforwardly found by substituting expressions (40) and (41) into Eqs. (37), (38), and (39). As in the case of zeroth-order solutions, these recursion relations are too cumbersome and will not be shown in this paper. Quantities $A^{(1)}_m$ and $B^{(1)}_m$ are first-order amplitudes to be calculated from boundary conditions. Finally, explicit expressions for $\mathbf{E}^{(1)}$ are easily obtained using Eqs. (28), (30), (40), and (41).

D. Boundary conditions: Light-scattering cross section

Let us calculate the amplitudes for both zeroth- and first-order fields. With this aim we apply Maxwell's boundary conditions at the surface $z=\zeta_r(\mathbf{r}_\parallel)$:

$$\hat{\boldsymbol{n}}\times\mathbf{E}^{-}(\mathbf{r}_\parallel,z)\big|_{z=\zeta_r}=\hat{\boldsymbol{n}}\times\mathbf{E}^{+}(\mathbf{r}_\parallel,z)\big|_{z=\zeta_r}, \tag{42}$$

$$\hat{\boldsymbol{n}}\times\mathbf{H}^{-}(\mathbf{r}_\parallel,z)\big|_{z=\zeta_r}=\hat{\boldsymbol{n}}\times\mathbf{H}^{+}(\mathbf{r}_\parallel,z)\big|_{z=\zeta_r}. \tag{43}$$

Here $-$ and $+$ superscripts correspond to the fields inside the vacuum and semiconductor, respectively, $\hat{\boldsymbol{n}}$ denotes a unit vector normal to the vacuum-semiconductor interface,

$$\hat{\mathbf{n}}=\left(-\frac{\partial\zeta_r(\mathbf{r}_\parallel)}{\partial x},-\frac{\partial\zeta_r(\mathbf{r}_\parallel)}{\partial y},1\right)\left[1+\left(\frac{\partial\zeta_r(\mathbf{r}_\parallel)}{\partial x}\right)^2+\left(\frac{\partial\zeta_r(\mathbf{r}_\parallel)}{\partial y}\right)^2\right]^{-1/2}. \tag{44}$$

In order to calculate all the amplitudes, it is necessary to apply the boundary condition for the excitonic polarization too,

$$\mathbf{P}(\mathbf{r}_\parallel,z)\big|_{z=\zeta_r}=\mathbf{0}. \tag{45}$$

The latter condition should not be considered a chosen ABC since it is a direct consequence of the vanishing of the exciton wave function at the surface. Expanding the vector $\hat{\boldsymbol{n}}$ in Eq. (44) and the fields $\mathbf{E}$, $\mathbf{H}$, and $\mathbf{P}$, appearing in boundary conditions [Eqs. (42), (43), and (45)], up to linear terms in $|\boldsymbol{\nabla}\zeta_r|\ll 1$, $k\delta_r\ll 1$, $\delta_r/a\ll 1$, and $\delta_f/a\ll 1$, we have obtained a system of algebraic equations for the amplitudes: $E^{(0)}_p(k_x)$ and $E^{(0)}_s(k_x)$ in Eq. (4), $E^{(1)}_p(\mathbf{k}'_\parallel)$ and $E^{(1)}_s(\mathbf{k}'_\parallel)$ in Eq. (6), $A^{(0)}_n$ in Eq. (24), $B^{(0)}_m$ in Eq. (25), $A^{(1)}_n$ in Eq. (40), and $B^{(1)}_m$ in Eq. (41) ($n=1,2$; $m=1,2,3$). The zeroth-order solutions of this system for the specific geometries of *s*- and *p*-polarized incident light coincide with those given in Refs. 39 and 40. In calculating the first-order amplitudes, it is convenient to write them in the form

$$\begin{aligned}
E^{(1)}_p(\mathbf{k}'_\parallel)&=E_{p,r}(\mathbf{k}'_\parallel)\zeta_r(\mathbf{k}'_\parallel-\mathbf{k}_\parallel)+E_{p,f}(\mathbf{k}'_\parallel)\zeta_f(\mathbf{k}'_\parallel-\mathbf{k}_\parallel),\\
E^{(1)}_s(\mathbf{k}'_\parallel)&=E_{s,r}(\mathbf{k}'_\parallel)\zeta_r(\mathbf{k}'_\parallel-\mathbf{k}_\parallel)+E_{s,f}(\mathbf{k}'_\parallel)\zeta_f(\mathbf{k}'_\parallel-\mathbf{k}_\parallel),\\
A^{(1)}_n(\mathbf{k}'_\parallel)&=A_{n,r}(\mathbf{k}'_\parallel)\zeta_r(\mathbf{k}'_\parallel-\mathbf{k}_\parallel)+A_{n,f}(\mathbf{k}'_\parallel)\zeta_f(\mathbf{k}'_\parallel-\mathbf{k}_\parallel),\\
B^{(1)}_m(\mathbf{k}'_\parallel)&=B_{m,r}(\mathbf{k}'_\parallel)\zeta_r(\mathbf{k}'_\parallel-\mathbf{k}_\parallel)+B_{m,f}(\mathbf{k}'_\parallel)\zeta_f(\mathbf{k}'_\parallel-\mathbf{k}_\parallel),
\end{aligned} \tag{46}$$

where $\zeta_r(\mathbf{k}'_\parallel)$ and $\zeta_f(\mathbf{k}'_\parallel)$ are the Fourier transforms of the surface profile $\zeta_r(\mathbf{r}_\parallel)$ and the function $\zeta_f(\mathbf{r}_\parallel)$, describing the surface potential fluctuations, respectively.

To determine the cross section of light-scattering into vacuum, we should also calculate the time- and ensemble-averaged Poynting vector of the first-order fields,[47,48,13]

$$\langle\mathbf{S}_{sc}\rangle=\frac{c}{8\pi}\langle\mathrm{Re}[\mathbf{E}^{(1)}_{sc}(\mathbf{r},t)^*\times\mathbf{H}^{(1)}_{sc}(\mathbf{r},t)]\rangle=\frac{c^2}{128\pi^5\omega}\int_{<}d^2k'_\parallel\int_{<}d^2k''_\parallel\,\langle\mathbf{E}^{(1)}_{sc}(\mathbf{k}''_\parallel)^*\times[\mathbf{K}'\times\mathbf{E}^{(1)}_{sc}(\mathbf{k}'_\parallel)]\rangle e^{i(\mathbf{K}'-\mathbf{K}'')\cdot\mathbf{r}}. \tag{47}$$

Here $\mathbf{K}'=\mathbf{k}'_\parallel-k'_z\hat{\mathbf{z}}$, the asterisk $*$ denotes the complex conjugate, and the symbol $<$ appended to the integrals indicates the region $k'_\parallel<\omega/c$, where k'_z is real, and then the fields propagate away from the sample surface. According to Eqs. (5), (6), and (46), the Fourier transform $\mathbf{E}^{(1)}_{sc}(\mathbf{k}'_\parallel)$ in Eq. (47) is given by

$$\mathbf{E}_{sc}^{(1)}(\mathbf{k}_\parallel')=\mathbf{E}_{sc,r}(\mathbf{k}_\parallel')\zeta_r(\mathbf{k}_\parallel'-\mathbf{k}_\parallel)+\mathbf{E}_{sc,f}(\mathbf{k}_\parallel')\zeta_f(\mathbf{k}_\parallel'-\mathbf{k}_\parallel), \tag{48}$$

where

$$\mathbf{E}_{sc,j}(\mathbf{k}_\parallel')=\hat{\mathbf{T}}[E_{p,j}(\mathbf{k}_\parallel')(\hat{\boldsymbol{x}}'\cos\theta'+\hat{\boldsymbol{z}}'\sin\theta') + E_{s,j}(\mathbf{k}_\parallel')\hat{\mathbf{y}}'], \quad j=r,f. \tag{49}$$

Thus, the Poynting vector (47) contains products $\zeta_j(\mathbf{k}_\parallel'')^*\zeta_{j'}(\mathbf{k}_\parallel')$ $(j=r,f;\ j'=r,f)$, which should be averaged. Because of the assumed statistical properties of the roughness and surface-potential fluctuations [see Eqs. (1), (11), and (12)], the ensemble average of the products $\zeta_j(\mathbf{k}_\parallel'')^*\zeta_{j'}(\mathbf{k}_\parallel')$ can be replaced by[14,16,48,50]

$$\langle\zeta_r(\mathbf{k}_\parallel'')\zeta_r(\mathbf{k}_\parallel')\rangle=4\pi^3\delta_r^2L_r^2\exp[-|\mathbf{k}_\parallel'|^2L_r^2/4]\delta(\mathbf{k}_\parallel'-\mathbf{k}_\parallel''),$$
$$\langle\zeta_f(\mathbf{k}_\parallel'')\zeta_f(\mathbf{k}_\parallel')\rangle=4\pi^3\delta_f^2L_f^2\exp[-|\mathbf{k}_\parallel'|^2L_f^2/4]\delta(\mathbf{k}_\parallel'-\mathbf{k}_\parallel''), \tag{50}$$
$$\langle\zeta_r(\mathbf{k}_\parallel'')\zeta_f(\mathbf{k}_\parallel')\rangle=4\pi^3\delta_r\delta_fL_rL_f\kappa_{rf}\exp[-|\mathbf{k}_\parallel'|^2L_{rf}^2/4]\times\delta(\mathbf{k}_\parallel'-\mathbf{k}_\parallel'').$$

Finally, the averaged Poynting vector $\langle\mathbf{S}_{sc}\rangle$ (47) acquires the form

$$\langle\mathbf{S}_{sc}\rangle=\frac{c^2}{32\pi^2\omega}\int_<d^2k_\parallel'\mathbf{K}'[|\mathbf{E}_{sc,r}|^2\delta_r^2L_r^2e^{-|\mathbf{k}_\parallel'-\mathbf{k}_\parallel|^2L_r^2/4} + |\mathbf{E}_{sc,f}|^2\delta_f^2L_f^2e^{-|\mathbf{k}_\parallel'-\mathbf{k}_\parallel|^2L_f^2/4} + 2\delta_r\delta_f\kappa_{rf}L_{rf}^2\,\mathrm{Re}(\mathbf{E}_{sc,r}^*\cdot\mathbf{E}_{sc,f})e^{-|\mathbf{k}_\parallel'-\mathbf{k}_\parallel|^2L_{rf}^2/4}]. \tag{51}$$

In addition, the time-averaged Poynting vector for the incident light is

$$\mathbf{S}_i=\frac{c}{8\pi}|E_i|^2[\hat{\boldsymbol{x}}\sin\theta_i+\hat{\boldsymbol{z}}\cos\theta_i]. \tag{52}$$

From Eqs. (51) and (52) we can calculate, in a standard way,[13,47–49] the dimensionless cross section $d\sigma/d\Omega$, which is defined as the ratio of the energy flux density of light scattered into the direction of $\mathbf{K}'$ to the energy flux density of the incident light per unit area of the surface $(\mathbf{S}_i\cdot\hat{\mathbf{z}})$. Using Eqs. (49), (51), and (52), we can express the cross section $d\sigma/d\Omega$ in terms of the amplitudes $E_{s,j}$ and $E_{p,j}$ $(j=r,f)$ corresponding to the *s* and *p* components of the first-order scattered field, respectively. Then,

$$\frac{d\sigma}{d\Omega}=\frac{\omega^2}{4\pi c^2}\frac{\cos\theta'}{\cos\theta_i}\frac{1}{|E_i|^2}\times\{[|E_{p,r}(\mathbf{k}_\parallel')|^2+|E_{s,r}(\mathbf{k}_\parallel')|^2]\times\delta_r^2L_r^2e^{-|\mathbf{k}_\parallel'-\mathbf{k}_\parallel|^2L_r^2/4}+[|E_{p,f}(\mathbf{k}_\parallel')|^2+|E_{s,f}(\mathbf{k}_\parallel')|^2]\delta_f^2L_f^2e^{-|\mathbf{k}_\parallel'-\mathbf{k}_\parallel|^2L_f^2/4}+2\delta_r\delta_f\kappa_{rf}L_{rf}^2\,\mathrm{Re}[E_{p,r}(\mathbf{k}_\parallel')^*E_{p,f}(\mathbf{k}_\parallel')+E_{s,r}(\mathbf{k}_\parallel')^*E_{s,f}(\mathbf{k}_\parallel')]e^{-|\mathbf{k}_\parallel'-\mathbf{k}_\parallel|^2L_{rf}^2/4}\}. \tag{53}$$

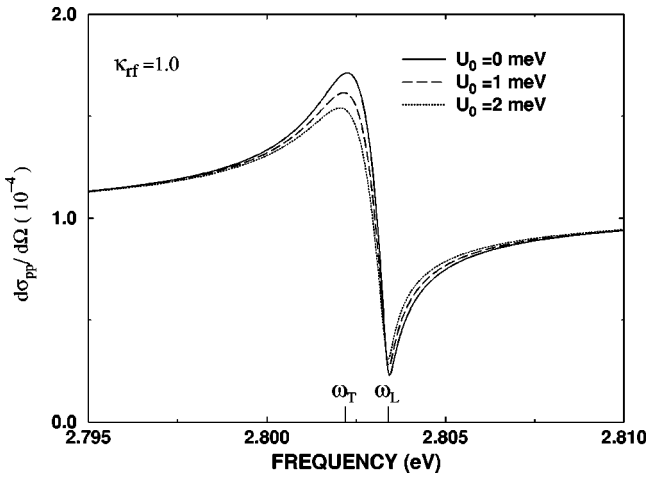

FIG. 1. Spectrum for the dimensionless cross section of light scattering, $d\sigma_{pp}/d\Omega$, from a ZnSe surface for *p*-polarized incident light at an angle of incidence $\theta_i=15°$ and angle of scattering in the plane of incidence $\theta'=3°$, with a correlation coefficient $\kappa_{rf}=1$. The values of the average height U_0 of the repulsive exponential potential are indicated in the figure.

Here, the terms with indices *s* and *p* describe the *s*- and *p*-polarized scattered power, respectively, within the differential solid angle $d\Omega=\sin\theta'd\theta'd\phi'$ $(k_x'=k\sin\theta'\cos\phi'$, $k_y'=k\sin\theta'\sin\phi'$, $k=\omega/c)$. Below, we will also use the symbol $d\sigma_{lq}/d\Omega$ to denote the component q $(q=s$ or $p)$ of the scattered power (53). In this notation the first index $(l=s$ or $p)$ indicates the polarization of the incident light.

We should point out that the form of $d\sigma/d\Omega$ [see Eq. (53)] is characteristic for scattering of light by two stochastic processes. The terms with δ_r^2 and δ_f^2 in Eq. (53) describe the power scattered from roughness and potential fluctuations, respectively. There is also a term with κ_{rf}, which determines the scattered power, associated with the cross-correlation between the random functions $\zeta_r(\mathbf{r}_\parallel)$ and $\zeta_f(\mathbf{r}_\parallel)$. The latter term would be zero if these random functions were statistically independent $(\kappa_{rf}=0)$. Expressions similar to Eq. (53) have been found, for example, in investigating light scattering from a rough surface with an inhomogeneous dielectric permittivity,[48] from the internal and external rough boundaries of an exciton-free layer,[13] and from an exciton quantum well with rough interfaces.[16]

III. REPULSIVE POTENTIALS

In this section we shall present numerical results for the dimensionless cross section $d\sigma/d\Omega$, considering that the exciton surface potential $U(\mathbf{r}_\parallel,z)$ is repulsive. As was mentioned in the Introduction, the intrinsic contributions to the surface potential, which are due to the no-escape boundary condition and the image potential,[20–22] repel excitons from the surface. Therefore, a semiconductor of sufficiently high quality and without surface treatment should be characterized, precisely, by a repulsive exciton surface potential.

Figures 1–5 show frequency and angle dependencies of $d\sigma/d\Omega$ calculated for ZnSe. In the calculation we used the parameters[51] $\epsilon_\infty=8.1$, $\hbar\omega_T=2.8022$ eV, $\hbar\omega_P=0.2334$ eV

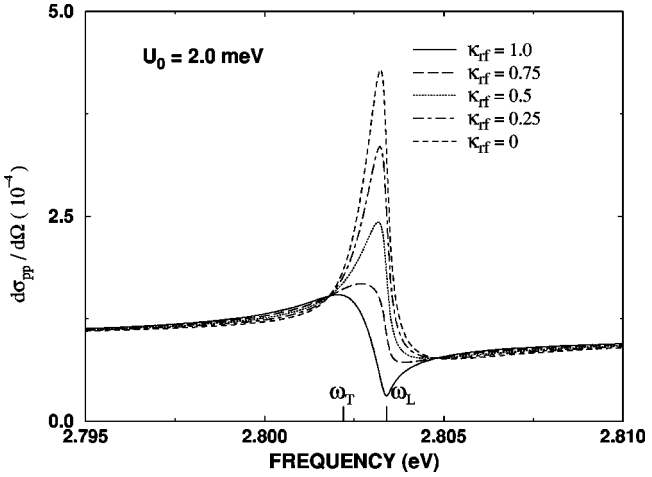

FIG. 2. The same as in Fig. 1, but with $U_0=2.0$ meV and distinct values of the correlation coefficient κ_{rf}.

(i.e., a longitudinal-transverse splitting $\hbar\omega_{LT}\approx\hbar\omega_P^2/2\omega_T\epsilon_\infty=1.2$ meV), and bulk damping $\hbar\nu=0.2$ meV. Here we employed the approximation of a single exciton branch with a total mass $M=0.57m$ (m is the free-electron mass), computed in Ref. 21. Since intrinsic transition layers are well described by the exponential model,[23,51–53] we used the surface potential (13) with the parameters

$$U_1=U_0,\quad U_2=0,\quad a=50\ \text{Å},\tag{54}$$

where U_0 denotes the average value (height) of the potential (13) at $z=0$ [$U_0=\langle U(\mathbf{r}_\parallel,0)\rangle=U(0)$]. Besides, we chose $\delta_r=\delta_f\equiv\delta$ ($\delta=8$ Å), $L_r=L_f=L_{rf}\equiv L$ ($L=2500$ Å). The numerical results presented in Figs. 1–5 consider scattering in the plane of incidence. According to our first-order calculations, for p- (s-) polarized incident light, there is only p- (s-) scattered light in the plane of incidence.

In the case of complete correlation between surface roughness and potential-well fluctuations, $\kappa_{rf}=1$, the frequency dependence of $d\sigma_{pp}/d\Omega$ (Fig. 1) and $d\sigma_{ss}/d\Omega$ look like the p- and s-polarization reflectivity spectra:[45,51] There is a maximum at the exciton-resonance frequency ω_T and a minimum at the longitudinal frequency ω_L. As the average height U_0 of the repulsive surface potential is increased, the maximum of $d\sigma_{pp}/d\Omega$ at ω_T decreases (see Fig. 1). We observed an analogous effect of U_0 on spectra $d\sigma_{ss}/d\Omega$ for s-polarized light.

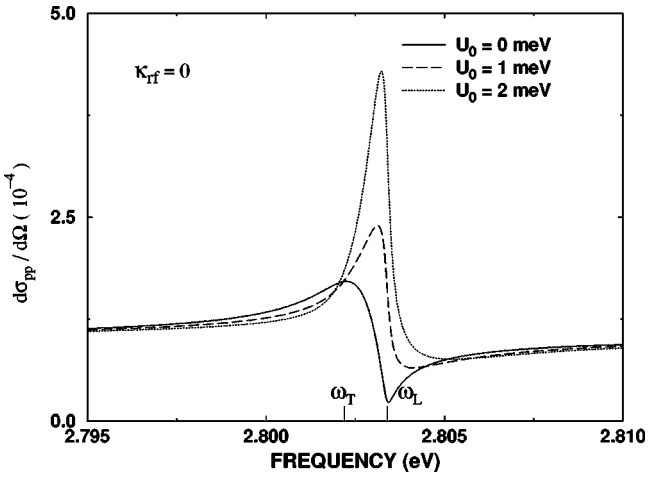

FIG. 3. The same as in Fig. 1, but with the correlation coefficient $\kappa_{rf}=0$.

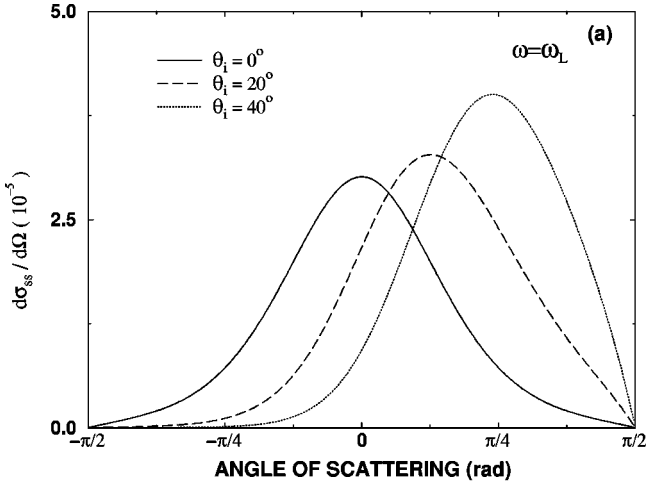

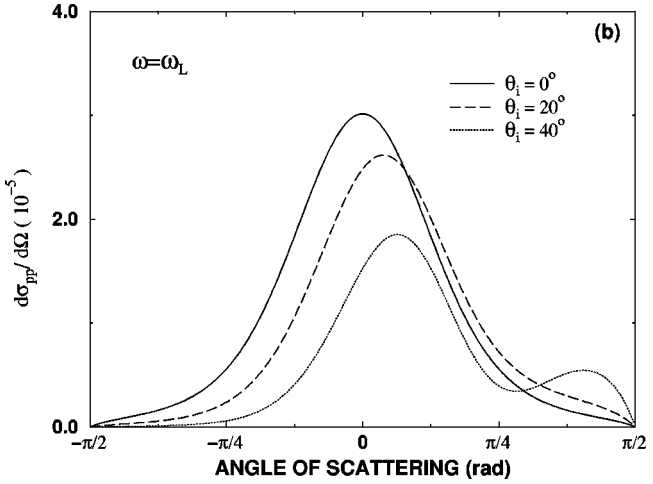

FIG. 4. Angular dependence of the dimensionless cross sections (a) $d\sigma_{ss}/d\Omega$ and (b) $d\sigma_{pp}/d\Omega$ for ZnSe calculated with the same sample parameters as in Figs. 1–3, $\omega=\omega_L$, $U_0=1$ meV, $\kappa_{rf}=1$ (complete correlation), and at different angles of incidence θ_i.

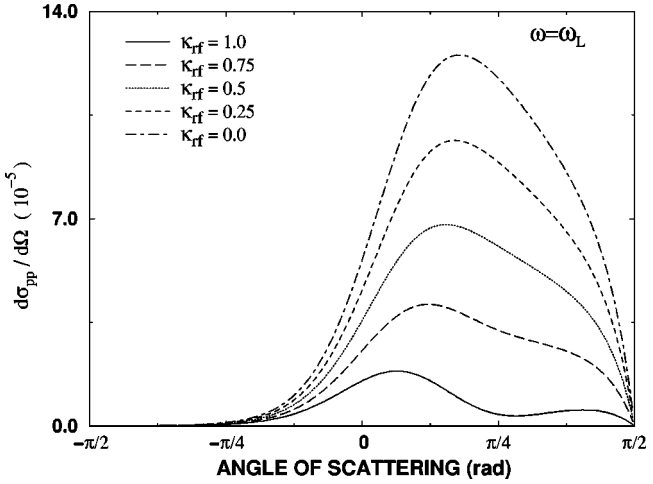

FIG. 5. Angular dependence of $d\sigma_{pp}/d\Omega$ for a ZnSe sample as in Figs. 1–3, $\omega=\omega_L$, $U_0=1$ meV, and $\theta_i=40°$. The values of the correlation coefficient κ_{rf} are indicated in the figure.

Impairing the correlation between $\zeta_r(\mathbf{r}_\parallel)$ and $\zeta_f(\mathbf{r}_\parallel)$, both $d\sigma_{pp}/d\Omega$ (Fig. 2) and $d\sigma_{ss}/d\Omega$ increase and a conspicuous peak near ω_L appears. This peak results from the fluctuations of the surface potential when they are not completely correlated with the profile of the rough surface (Fig. 2) and increases with U_0 (Fig. 3). According to the formula (53), the spectral line shape of $d\sigma/d\Omega$ with $\kappa_{rf}\approx 0$ is mainly determined by the terms associated with scattering from surface roughness and potential fluctuations since the cross-correlation term can be neglected. However, when the correlation coefficient is not very small ($\kappa_{rf}\lesssim 1$), the cross-correlation term of $d\sigma/d\Omega$ [Eq. (53)], which turns out to be negative, competes with the other terms and can drastically modify the light-scattering spectra (see Fig. 2).

Angle dependencies of $d\sigma/d\Omega$, calculated in the case of complete correlation ($\kappa_{rf}=1$) and at different angles of incidence θ_i, are shown in Fig. 4. It can be seen that the *maximum* of $d\sigma_{ss}/d\Omega$ [Fig. 4(a)] is close to the specular direction. As the angle of scattering goes away from this direction, $d\sigma_{ss}/d\Omega$ decreases monotonically. The angle dependence of $d\sigma_{pp}/d\Omega$ is analogous to that of $d\sigma_{ss}/d\Omega$ within the whole frequency region of the exciton resonance, except at the longitudinal frequency ω_L. So, with $\omega=\omega_L$ and $\kappa_{rf}=1$, the angular dependence of $d\sigma_{pp}/d\Omega$ exhibits a *minimum* near the specular direction at relatively large angles of incidence [see the curve in Fig. 4(b) for $\theta_i=40°$]. This surprising result can only be attributed to the excitation of the longitudinal mode in the *p*-polarization geometry. Decreasing κ_{rf}, the angular dependence of $d\sigma_{pp}/d\Omega$ at $\omega=\omega_L$ is modified so that its minimum near the specular direction becomes a maximum (see Fig. 5).

Now, let us apply the theory developed in the preceding section to a CdS semiconductor. The interest in this kind of semiconductor is due to the fact that its spectra of elastic scattering of light have already been investigated both experimentally and theoretically in several works.[10–15] So, we can verify how well our theory explains experimental results. Figure 6(a) presents experimental spectra of $d\sigma_{pp}/d\Omega$ for CdS in the region of the $A_{n=1}$ exciton state, which were taken from Ref. 13. In this work the distinct spectral curves of $d\sigma_{pp}/d\Omega$ were obtained from different areas of the same crystal surface with angles of incidence and scattering, $\theta_i=14°$ and $\theta'=4°$, respectively. Curve 1 in Fig. 6(a) has a single maximum at the longitudinal frequency $\omega=\omega_L$. This type of spectrum is very common and has been observed in a great variety of high-quality CdS samples.[10–15] However, in some cases the line shape of the spectrum $d\sigma_{pp}/d\Omega$ is quite different from the curve 1 in Fig. 6(a), since, in addition to the maximum at ω_L, there is another maximum near the exciton resonance frequency[11,13] ω_T [compare curves 3 and 4 with curve 1 in Fig. 6(a)]. These experimental spectra were explained in Ref. 13 as a result of light scattering not only by the roughness of the crystal surface but also by the fluctuations of the surface excitonic potential. In the theory[13] the repulsive exciton potential was approximated by a 70 Å dead layer, applying the Pekar ABC for the excitonic polarization $\mathbf{P}$ [i.e., $\mathbf{P}=0$ (Ref. 19)] at its inner rough boundary.

Our theoretical results for $d\sigma_{pp}/d\Omega$ [Fig. 6(b)], obtained by modeling the excitonic surface potential as a repulsive exponential one, accomplish a quantitative reproduction of the experimental spectra of Fig. 6(a). This fit turns out to be much better than that of Ref. 13, where the dead-layer model was applied. In our calculations we fixed various CdS parameters[54] $\hbar\omega_P=0.293\,96$ eV, $\epsilon_\infty=9.1$, $M=0.94m$, $\hbar\nu=0.124$ meV, and found the best fit for $\hbar\omega_T=2.552\,25$ eV. This value of ω_T is very close to those used in Refs. 13, 21, and 51 and is in reasonable agreement with other values reported in the literature.[54–56] The repulsive surface potential is given by Eqs. (13) and (54) with the parameters $U_0=4$ meV and $a=70$ Å, which have also allowed to reproduce satisfactorily the specular reflectivity of CdS (near $A_{n=1}$ exciton resonance) for *p*-polarized light at 9° angle of incidence, presented in Ref. 14. The statistical parameters for the surface profile and the potential fluctuations are indicated in the caption of Fig. 6.

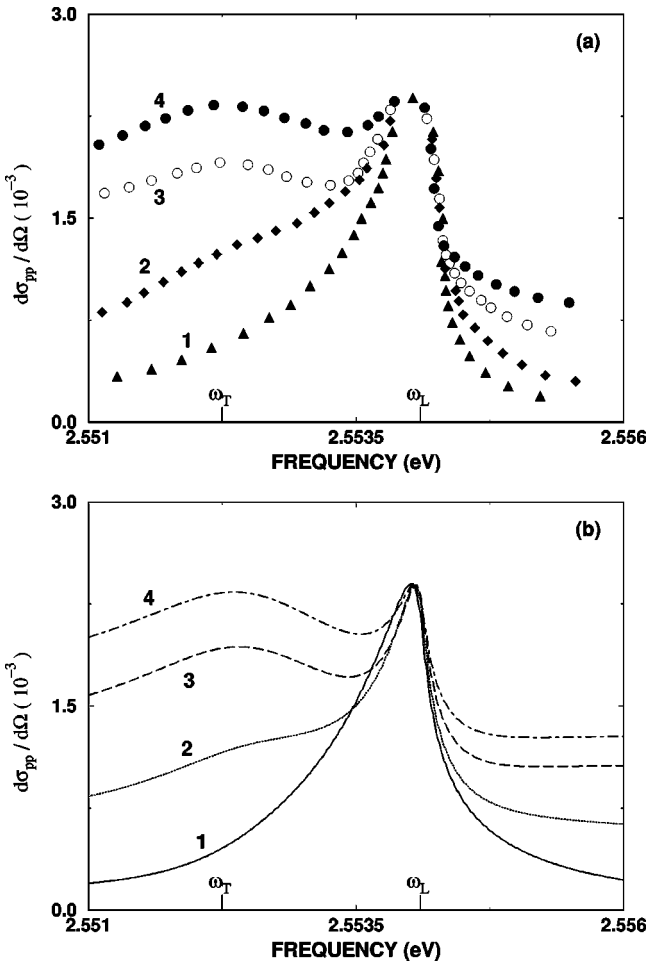

FIG. 6. (a) Experimental data for the dimensionless cross section $d\sigma_{pp}/d\Omega$ of CdS taken from Ref. 13. Graphs 1–4 correspond to light-scattering cross section measured at angles of incidence $\theta_i=14°$ and scattering $\theta'=4°$ and on different areas of the same crystal surface, being parallel to the hexagonal **c** axis. (b) Theoretical spectra for the dimensionless light-scattering cross section of CdS, calculated with a repulsive (exponential) potential. The statistical parameters for the rough surface and the fluctuations of the surface potential are: $\delta_r=5.05$ Å, $\delta_f=11.35$ Å ($\eta=0.38$), $\kappa_{rf}=0.39$ (curve 1); $\delta_r=10.45$ Å, $\delta_f=21.55$ Å ($\eta=0.34$), $\kappa_{rf}=0.917$ (curve 2); $\delta_r=15.1$ Å, $\delta_f=26.05$ Å ($\eta=0.27$), $\kappa_{rf}=0.931$ (curve 3); $\delta_r=17.8$ Å, $\delta_f=26.2$ Å ($\eta=0.19$), $\kappa_{rf}=0.915$ (curve 4); the correlation lengths L_r, L_f, and L_{rf} are the same for all the curves ($L_r=L_f=L_{rf}=0.5$ μm).

Note that the spectra with maxima at both ω_L and ω_T

[curves 3 and 4 in Fig. 6(b)] were calculated by using a large correlation coefficient κ_{rf} (>0.9) and close values for δ_r and δ_f [$\eta \equiv |\delta_f - \delta_r|/(\delta_f + \delta_r) < 0.3$]. On the other hand, the spectrum of light scattering corresponding to a smaller value of the correlation coefficient ($\kappa_{rf} = 0.39$) and a larger quantity η ($=0.38$) has a single maximum at ω_L [see curve 1 in Fig. 6(b)]. An intermediate situation is observed in spectrum 2 of Fig. 6(b), which exhibits a shoulder at the frequency ω_T and a prominent peak at ω_L. These results show that the line shape of light-scattering spectra depends strongly on the degree of correlation between the potential fluctuations and the surface roughness in the irradiated areas of the sample.

Finally, we should comment that there exist other mechanisms (substantial increase of the transition-layer thickness and decrease of damping[23,57]) that produce a peak in the specular reflectivity near the longitudinal frequency ω_L and might also modify the line shape of light-scattering spectra. However, in interpreting the experiment[13] we have excluded such mechanisms because they would require the use of unrealistic parameters (a and ν) for the CdS sample, from which the spectra of Fig. 6(a) were obtained. Therefore, we can affirm that the form of the experimental curves [Fig. 6(a)] is principally produced by the effect of the correlation between surface roughness and potential fluctuations.

IV. NEAR-SURFACE LOCALIZED EXCITONS

Now, let us analyze the scattering of light from semiconductors with an extrinsic near-surface potential well. Figures 7–10 show frequency and angle dependencies of $d\sigma/d\Omega$ for ZnSe, which were calculated by using the same parameters for the sample (ω_T, ω_P, ϵ_∞, M, ν, $\delta_r = \delta_f$, $L_r = L_f = L_{rf}$) as in Figs. 1–5. Hereafter, the surface potential $U(\mathbf{r}_\parallel, z)$ with small random fluctuations in Eq. (13) is modeled by employing a truncated Morse potential:[39,40,45]

$$U_1 = -2|U_m| e^{z_m/a}, \quad U_2 = |U_m| e^{2z_m/a}, \tag{55}$$

where $|U_m|$ symbolizes the depth of the average potential well, which coincides with the potential well for a flat surface ($\langle U(\mathbf{r}_\parallel, z)\rangle = U(z) = U_1 e^{-z/a} + U_2 e^{-2z/a}$); z_m is the position of its minimum [$U_m = U(z_m)$]. The effective width of the potential well $U(z)$ is approximately $2.3a$.[39] The parameters of the extrinsic potential in Eq. (55), used here, are $U_m = -1$ meV, $z_m = 150$ Å, and $a = 150$ Å. According to the chosen parameters, the average potential well $U(z)$ has two excitonic bound states at $\hbar\omega_{T1} = 2.8017$ eV, and $\hbar\omega_{T2} = 2.802\,17$ eV which, as is usual,[39,40,45] are calculated from the Schrödinger equation for the translational motion of the exciton,

$$\frac{\hbar^2}{2M}\left(k_x^2 - \frac{\partial^2}{\partial z^2}\right)\psi(z) + [\hbar\omega_T + U(z)]\psi(z) - \hbar\omega\psi(z) = 0, \tag{56}$$

with the boundary conditions $\psi(0) = 0$ and $\psi(\infty) = 0$. It should be noted that the first term on the left-hand side of Eq. (56) gives a negligible contribution to the eigenvalues $\hbar\omega_{Tn}$, which is of the order of 10^{-5} eV. As was mentioned in the Introduction, the presence of near-surface localized excitons leads to the generation of quantized longitudinal polarization waves.[44,40] These modes satisfy the condition of vanishing of the displacement vector, $\mathbf{D} = \varepsilon_\infty \mathbf{E} + 4\pi\mathbf{P} = \mathbf{0}$. Hence, the longitudinal polaritonic fields of zeroth order, satisfying $\mathbf{D}^{(0)} = \mathbf{0}$, should obey the equation

$$\frac{\hbar^2}{2M}\left(k_x^2 - \frac{\partial^2}{\partial z^2}\right)\mathbf{P}^{(0)}(k_x, z) + [\hbar\omega_T + \hbar\omega_{LT} + U(z)] \times \mathbf{P}^{(0)}(k_x, z) - \hbar\omega\mathbf{P}^{(0)}(k_x, z) = \mathbf{0}, \tag{57}$$

which is straightforwardly obtained from Eq. (16) if we omit there the damping term and consider that the differences between ω, ω_T, and ω_L are small. Comparing Eqs. (56) and (57), we see that the eigenenergies of the quantized longitudinal modes are shifted with respect to the eigenvalues of the excitonic bound states: $\hbar\omega_{L1} = \hbar(\omega_{T1} + \omega_{LT}) = 2.8029$ eV, $\hbar\omega_{L2} = \hbar(\omega_{T2} + \omega_{LT}) = 2.803\,37$ eV. On the other hand, the

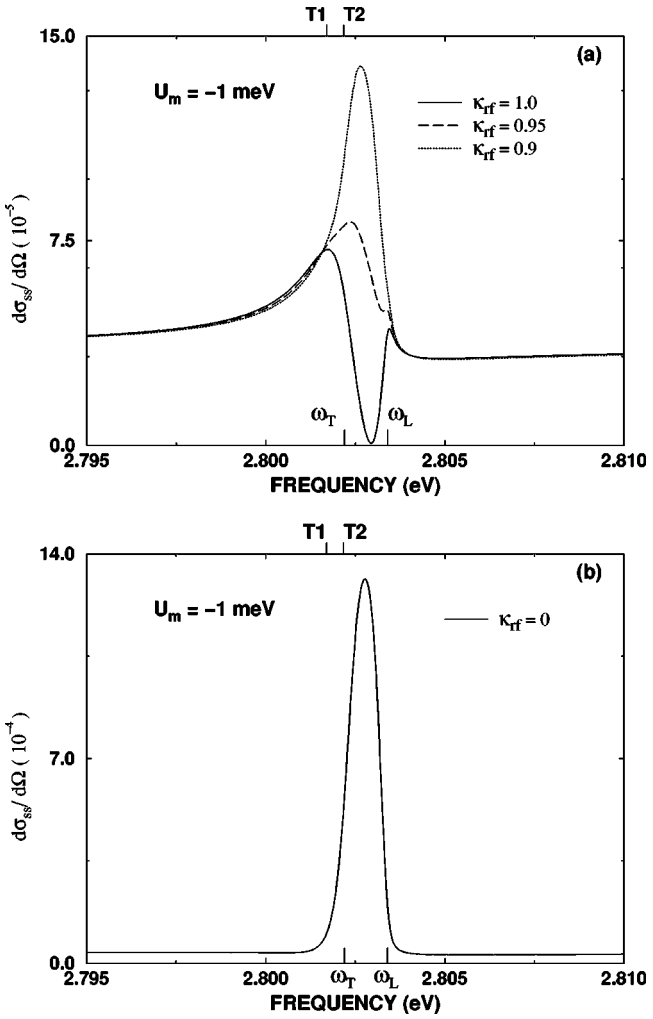

FIG. 7. Spectrum of the dimensionless cross section of light scattering from a ZnSe surface in the presence of two localized excitons. The incident light is s polarized with an angle of incidence $\theta_i = 40°$, and the scattered light is s polarized in the plane of incidence with $\theta' = 3°$. The values of the correlation coefficient k_{rf} are: 1, 0.95 , 0.9 in panel (a), and 0 in panel (b).

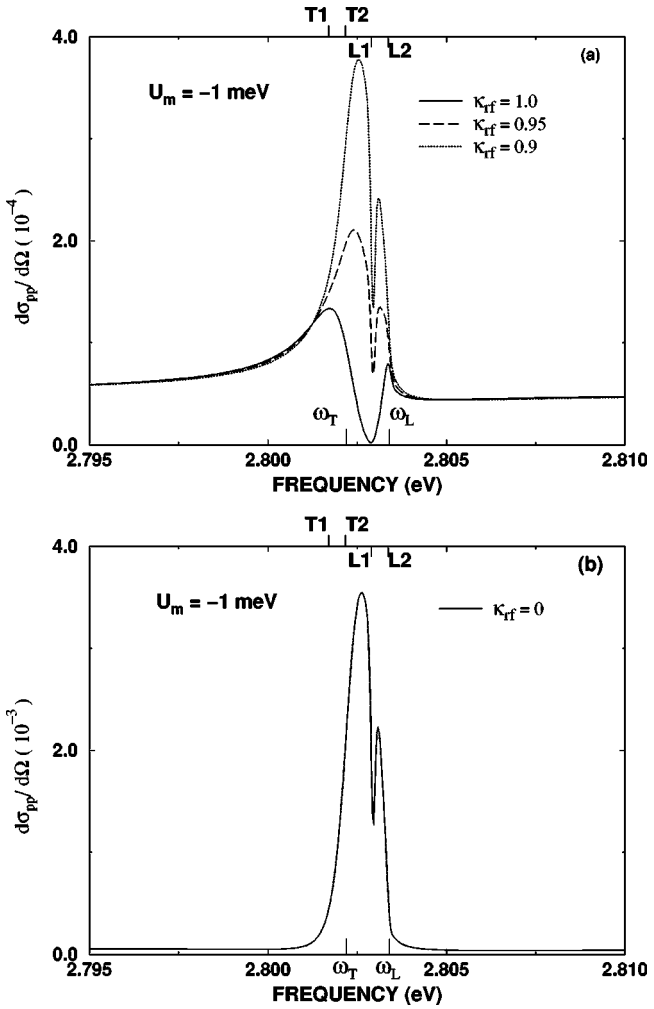

FIG. 8. Spectrum of the dimensionless cross section of light scattering from a ZnSe surface in the presence of two localized excitons. The incident light is *p* polarized with an angle of incidence $\theta_i = 40°$, and the scattered light is *p* polarized in the plane of incidence with $\theta' = 35°$. The values of the correlation coefficient k_{rf} are 1, 0.95, 0.9 in panel (a), and 0 in panel (b).

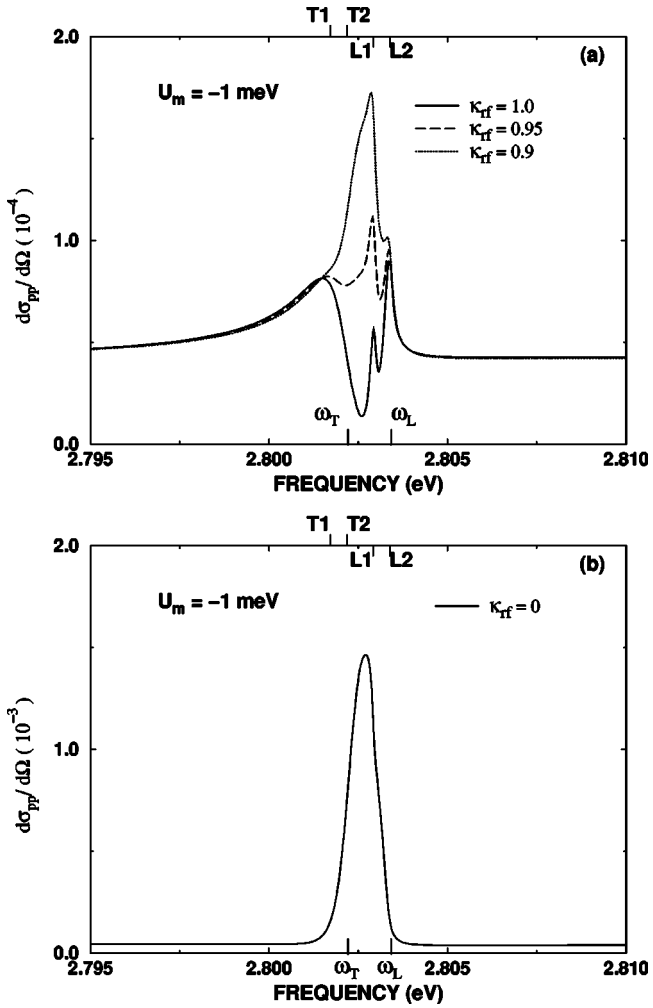

FIG. 9. The same as in Fig. 8, but the angle of scattering $\theta' = 3°$.

longitudinal modes of the scattered polaritonic fields inside the sample satisfy the equation

$$\frac{\hbar^2}{2M}\left((k'_{\parallel})^2 - \frac{\partial^2}{\partial z^2}\right)\mathbf{P}^{(1)}(\mathbf{k}'_{\parallel},z) + [\hbar\omega_T + \hbar\omega_{LT} + U(z)] \times \mathbf{P}^{(1)}(\mathbf{k}'_{\parallel},z) - \hbar\omega\mathbf{P}^{(1)}(\mathbf{k}'_{\parallel},z) = \frac{\hbar^2}{2M}\mathbf{F}(\mathbf{k}'_{\parallel},z). \quad (58)$$

Indeed, using formulas (29) and (35), and the condition $\mathbf{D}^{(1)} = 0$ for the longitudinal modes of the first-order fields, Eq. (18) for $\mathbf{E}^{(1)}$ and $\mathbf{P}^{(1)}$ can be rewritten in the form (58). Note that the reduced equation of the inhomogeneous one (58) is precisely Eq. (57), with the quantities k_x and $\mathbf{P}^{(0)}$ replaced by $k'_{\parallel}$ and $\mathbf{P}^{(1)}$, respectively. Therefore, the first-order polaritonic fields should have a resonant behavior at frequencies very close to the eigenvalues ω_{Ln}. It means that singularities, associated with the quantized longitudinal modes, should appear in the spectra of light scattering. This statement is verified by our numerical results, which are discussed below.

Figures 7–10 correspond to light scattering in the plane of incidence. We remind readers that, according to our first-order perturbation theory, the scattered light in the plane of incidence has the same polarization (*p* or *s*) of the incident light. In the case of complete correlation between surface roughness and potential-well fluctuations, $k_{rf} = 1$, the dependence of $d\sigma_{ss}/d\Omega$ on frequency [Fig. 7(a)] resembles the *s*-polarization reflectivity spectrum:[45] The maximum (broad peak) of $d\sigma_{ss}/d\Omega$ below ω_T is produced by the bulk exciton resonance (T) together with transverse resonances ($T1$ and $T2$) associated with near-surface localized excitons. As the coefficient of correlation tends to zero ($k_{rf} \to 0$), $d\sigma_{ss}/d\Omega$ increases considerably in the interval $\omega_T < \omega < \omega_L$ [Fig. 7(b)]. It is interesting that this effect of the correlation coefficient on the light-scattering cross section is similar to that found in the case of repulsive (intrinsic) potentials (see Sec. III).

The spectrum of $d\sigma_{pp}/d\Omega$ for *p*-polarized light depends strongly on the angle of scattering θ' [Figs. 8 and 9]. When $k_{rf} = 1$ and θ' is close to the angle corresponding to the

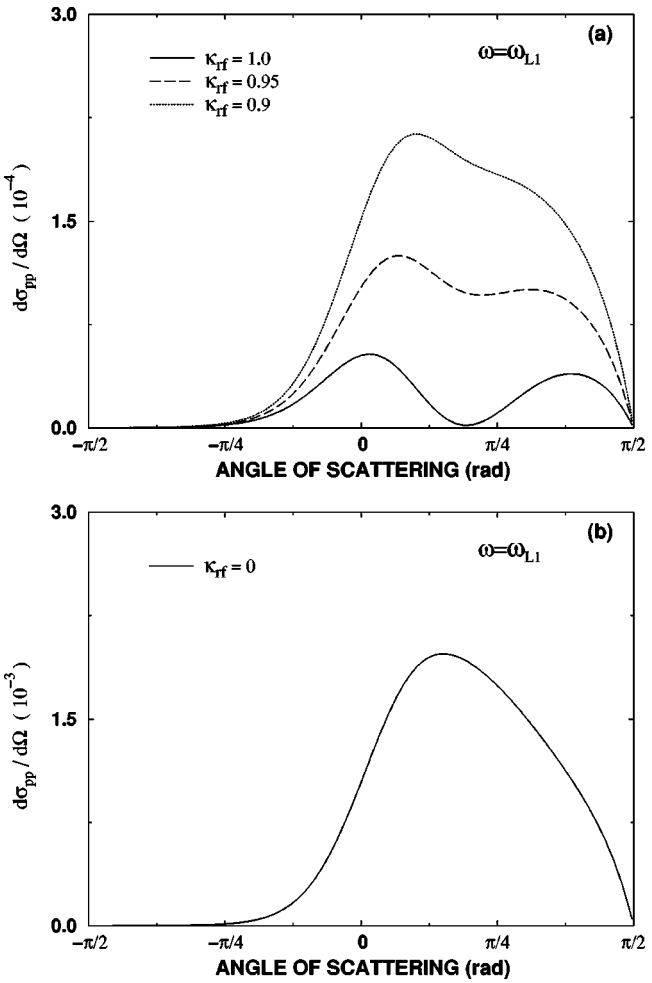

FIG. 10. Angular dependence of the dimensionless cross section $d\sigma_{pp}/d\Omega$ for ZnSe calculated with the same parameters as in Fig. 8, and with $\omega=\omega_{L1}$.

specular direction, $d\sigma_{pp}/d\Omega$ (Fig. 8(a)) reproduces the same features of the *p*-polarization reflectivity.[45] Diminishing the correlation between the random functions $\zeta_r(\mathbf{r}_\parallel)$ and $\zeta_f(\mathbf{r}_\parallel)$, $d\sigma_{pp}/d\Omega$ increases notably [see Fig. 8(b)] and the longitudinal resonance at ω_{L1}, associated with the deepest level $(n=1)$ of the quantized polarization waves, is clearly observed as a dip. Sufficiently far from the specular direction, the longitudinal resonances manifest themselves as peaks in the spectrum $d\sigma_{pp}/d\Omega$ at frequencies ω_{L1} and ω_{L2} (see Fig. 9). These results confirm our predictions, namely, the presence of quantized longitudinal polarization waves in the scattered polaritonic fields and their resonant manifestation in spectra of light scattering. We should mention that the surface damping in an extrinsic transition layer is larger than the bulk damping and, therefore, the resonances, associated with the near-surface localized excitons, in spectra of light scattering can be smoothed out and two or more of them may coalesce into a single one. This fact should be taken into account in interpreting experimental spectra.[40]

Another interesting manifestation of the quantized longitudinal polarization modes can be observed in the angular dependence of $d\sigma_{pp}/d\Omega$ shown in Fig. 10. As is seen there, the scattering cross section at the frequency $\omega=\omega_{L1}$ of the first quantized longitudinal mode has a minimum near the specular direction when the value of the coefficient k_{rf} is close to one (complete correlation). This angular dependence [Fig. 10(a)] looks like that of $d\sigma_{pp}/d\Omega$ for a sample with an intrinsic potential at the frequency ω_L of the bulk longitudinal mode [compare with the curve labeled with $\kappa_{rf}=1$ in Fig. 5(a)]. As the correlation coefficient κ_{rf} decreases, the minimum of $d\sigma_{pp}/d\Omega$ near the specular direction becomes a maximum (see Fig. 10).

We have also calculated spectra of $d\sigma/d\Omega$ for CdS and GaAs (Ref. 46) samples in the presence of an extrinsic near-surface potential well. The generation of excitonic bound states within the potential well leads to resonances in their light-scattering spectra. Besides, as in the case of ZnSe, the decrease of the correlation between the profile of the rough surface and the potential-well fluctuations produces a considerable increase of $d\sigma/d\Omega$ in the frequency region $\omega_T<\omega<\omega_L$.

V. CONCLUSION

We have developed a perturbation theory for describing the phenomenon of light scattering from semiconductor rough surfaces near exciton resonance. In our theory we have modeled the interaction between the exciton and the rough surface by means of a generalized Morse potential with random fluctuations. This model allows to study the effect of both intrinsic (repulsive) transition layers and near-surface (extrinsic) potential wells on spectra of light scattering. In both cases, the light-scattering cross section increases substantially near the longitudinal frequency ω_L as the correlation between the profile of the rough surface and the fluctuations of the surface potential decreases. Applying this theory, we could quantitatively reproduce experimental spectra of light-scattering cross section for CdS samples of sufficiently high quality.

It was also shown that the presence of exciton bound states within a near-surface potential well affects notably both frequency and angle dependencies of the light-scattering cross section. In particular, the longitudinal modes associated with the near-surface localized excitons produce resonances in spectra of diffuse reflection, which are intensified as the correlation between the surface roughness and the potential-well fluctuations diminishes. The optical manifestation of such longitudinal confined modes turned out to be very sensitive not only to the angle of incidence, but also to the angle of scattering.

Because of the large number of parameters to be specified in the theory, spectra of light-scattering cross section as well as specular reflectivity[19,39,51] can be reproduced by different sets of parameters. Therefore, it is recommendable to determine first the parameters of the average surface potential from various reflectivity measurements (for example, at different angles of incidence for both *s* and *p* polarizations). Afterwards, the statistical parameters for the surface profile and potential fluctuations can be adjusted to experimental spectra of diffuse reflection.

Finally, we should emphasize that the theory developed in this work is based on the adiabatic approach[19] and has a phenomenological character due to the use of an excitonic

surface potential with fitting parameters. The employment of this phenomenological theory is well justified by the clear and simple interpretation of experiments on light scattering. Nevertheless, it would be also interesting to compare our results with predictions of microscopic theories (for example, the analytical-variational approach by D'Andrea and Del Sole,[21,58] ABC-free theory of Cho,[59,60] and Stahl's coherent wave approach[61–63]), which have been mostly applied to investigate optical properties of excitonic media with ideally flat surfaces.

ACKNOWLEDGMENTS

This work was partially supported by the Consejo Nacional de Ciencia y Tecnología (CONACYT) under Grant No. 26184-E. F.P.-R. is grateful to A. V. Sel'kin, V. A. Kosobukin, and N. M. Makarov for stimulating discussions.

[1] Nieto-Vesperinas, *Scattering and Diffraction in Physical Optics* (Wiley, New York, 1991).
[2] J. A. Ogilvy, *Theory of Wave Scattering from Random Rough Surfaces* (Hilger, Bristol, 1991).
[3] K. V. Sobha and G. S. Agarwal, Solid State Commun. **43**, 99 (1982).
[4] G. S. Agarwal and C. V. Kunasz, Phys. Rev. B **26**, 5832 (1982).
[5] S. Wang, R. G. Barrera, and W. L. Mochán, Phys. Rev. B **40**, 1571 (1989).
[6] S. Wang, W. L. Mochán, and R. G. Barrera, Phys. Rev. B **42**, 9155 (1990).
[7] S. Wang, J. Siqueiros, and R. Machorro, Opt. Commun. **122**, 9 (1995).
[8] E. L. Albuquerque, N. S. Almeida, and M. C. Oliveros, Phys. Status Solidi B **129**, 177 (1985).
[9] G. H. Cocoletzi and S. Wang, Phys. Rev. B **48**, 17 413 (1993).
[10] A. B. Pevtsov, S. A. Permogorov, and A. V. Sel'kin, Pis'ma Zh. Éksp. Teor. Fiz. **33**, 419 (1981) [JETP Lett. **33**, 402 (1981)].
[11] A. B. Pevtsov and A. V. Sel'kin, Fiz. Tverd. Tela (Leningrad) **26**, 2875 (1984) [Sov. Phys. Solid State **26**, 1741 (1984)].
[12] V. A. Kosobukin and A. V. Sel'kin, Pis'ma Zh. Éksp. Teor. Fiz. **44**, 377 (1986) [JETP Lett. **44**, 483 (1986)].
[13] V. A. Kosobukin and A. V. Sel'kin, Solid State Commun. **66**, 313 (1988).
[14] V. A. Kosobukin, M. I. Sazhin, and A. V. Sel'kin, Fiz. Tverd. Tela (Leningrad) **32**, 1023 (1990) [Sov. Phys. Solid State **32**, 602 (1990)].
[15] V. A. Kosobukin, M. I. Sazhin, and A. V. Sel'kin, Solid State Commun. **94**, 947 (1995).
[16] V. A. Kosobukin, Solid State Commun. **108**, 83 (1998).
[17] D. Franta and I. Ohlídal, J. Mod. Opt. **45**, 903 (1998).
[18] *Spatial Dispersion in Solids and Plasmas*, edited by P. Halevi, Electromagnetic Waves–Recent Developments in Research, Vol. 1 (Elsevier, Amsterdam, 1992).
[19] See, for example, *Spatial Dispersion in Solids and Plasmas* (Ref. 18), Chap. 6.
[20] I. Balslev, Phys. Status Solidi B **88**, 155 (1978).
[21] A. D'Andrea and R. Del Sole, Phys. Rev. B **25**, 3714 (1982).
[22] J. J. Hopfield and D. G. Thomas, Phys. Rev. **132**, 563 (1963).
[23] I. Balslev, Phys. Rev. B **23**, 3977 (1981).
[24] A. S. Batyrev, N. V. Karasenko, and A. V. Sel'kin, Fiz. Tverd. Tela (St. Petersburg) **35**, 3099 (1993) [Phys. Solid State **35**, 1525 (1993)].
[25] A. S. Batyrev, B. V. Novikov, and A. V. Sel'kin, Pis'ma Zh. Éksp. Teor. Fiz. **61**, 791 (1995) [JETP Lett. **61**, 809 (1995)].
[26] A. S. Batyrev, A. E. Cherednichenko, and V. A. Kiselev, Fiz. Tverd. Tela (Leningrad) **29**, 2126 (1987) [Sov. Phys. Solid State **29**, 1221 (1987)].
[27] V. N. Ermakov, D. V. Korbutyak, V. G. Litovchenko, O. Yu. Mikityuk, and V. V. Nitsovich, Phys. Status Solidi B **125**, 815 (1984).
[28] P. Gueétin and G. Schrédr, J. Appl. Phys. **43**, 549 (1972).
[29] L. H. Dubois and B. R. Zegarski, Phys. Rev. B **35**, 9128 (1987).
[30] V. A. Kiselev, B. V. Novikov, E. A. Ubushiev, S. S. Utnasunov, and A. E. Cherednichenko, Pis'ma Zh. Éksp. Teor. Fiz. **43**, 371 (1986) [JETP Lett. **43**, 476 (1986)].
[31] V. A. Kiselev, B. V. Novikov, A. E. Cherednichenko, and E. A. Ubushiev, Phys. Status Solidi B **133**, 573 (1986).
[32] L. Schultheis and J. Lagois, Phys. Rev. B **29**, 6784 (1984), and references therein.
[33] J. Lagois, E. Wagner, W. Bludau, and K. Lösch, Phys. Rev. B **18**, 4325 (1978).
[34] F. Evangelisti, A. Frova, and F. Patella, Phys. Rev. B **10**, 4253 (1974).
[35] F. Evangelisti, J. U. Fischbach, and A. Frova, Phys. Rev. B **9**, 1516 (1974).
[36] V. A. Kiselev, B. V. Novikov, A. S. Batyrev, E. A. Ubushiev, and A. E. Cherednichenko, Phys. Status Solidi B **135**, 597 (1986), and references therein.
[37] A. E. Cherednichenko and V. A. Kiselev, Prog. Surf. Sci. **36**, 179 (1991).
[38] A. S. Batyrev, V. A. Kiselev, B. V. Novikov, and A. E. Cherednichenko, Pis'ma Zh. Éksp. Teor. Fiz. **39**, 436 (1984) [JETP Lett. **39**, 528 (1984)].
[39] F. Pérez-Rodríguez and P. Halevi, Phys. Rev. B **45**, 11 854 (1992).
[40] F. Pérez-Rodríguez and P. Halevi, Phys. Rev. B **53**, 10 086 (1996).
[41] P. Halevi and F. Pérez-Rodríguez, Fiz. Nizk. Temp. **18**, 1135 (1992) [Sov. J. Low Temp. Phys. **18**, 795 (1992)].
[42] B. Flores-Desirena, F. Pérez-Rodríguez, and P. Halevi, Phys. Rev. B **50**, 5404 (1994).
[43] H. A. Coyotécatl and G. H. Cocoletzi, J. Phys.: Condens. Matter **10**, 79 (1998).
[44] F. Pérez-Rodríguez and P. Halevi, Phys. Rev. B **48**, 2016 (1993).
[45] J. Madrigal-Melchor, F. Pérez-Rodríguez, J. A. Maytorena, and W. L. Mochán, Appl. Phys. Lett. **71**, 69 (1997).
[46] J. Madrigal-Melchor, F. Pérez-Rodríguez, A. Silva-Castillo, and H. Azucena-Coyotécatl, Fiz. Tverd. Tela (St. Petersburg) **40**, 865 (1998) [Phys. Solid State **40**, 796 (1998)].
[47] A. A. Maradudin and D. L. Mills, Phys. Rev. B **11**, 1392 (1975).
[48] J. M. Elson, Phys. Rev. B **30**, 5460 (1984).
[49] J. M. Elson, Phys. Status Solidi B **62**, 461 (1974).
[50] A. A. Maradudin, Jun Q. Lu, P. Tran, R. F. Wallis, V. Celli, Zu-Han Gu, A. R. McGurn, E. R. Méndez, T. Michel, M. Nieto-Vesperinas, J. C. Dainty, and A. J. Sant, Rev. Mex. Fis. **38**, 343 (1992).
[51] R. Ruppin, Phys. Rev. B **29**, 2232 (1984).

[52] R. Ruppin and R. Englman, Phys. Rev. Lett. **53**, 1688 (1984).
[53] E. G. Skaistis and V. N. Khotyaintsev, Fiz. Tverd. Tela (Leningrad) **24**, 3648 (1982) [Sov. Phys. Solid State **24**, 2079 (1982)].
[54] P. Y. Yu and F. Evangelisti, Phys. Rev. Lett. **42**, 1642 (1979).
[55] J. Lagois, Phys. Rev. B **16**, 1699 (1977).
[56] J. Lagois, Phys. Rev. B **23**, 5511 (1981).
[57] F. Evangelisti, A. Frova, and F. Patella, Phys. Rev. B **10**, 4253 (1974).
[58] A. D'Andrea and R. Del Sole, Phys. Rev. B **38**, 1197 (1988).
[59] K. Cho, J. Phys. Soc. Jpn. **55**, 4113 (1986).
[60] K. Cho and H. Ishihara, in *Excitons in Confined Systems*, edited by R. Del Sole, A. D'Andrea, and A. Lapiccirella (Springer-Verlag, Berlin, 1988), p. 90.
[61] A. Stahl and I. Balslev, *Electrodynamics of the Semiconductor Band Edge* (Springer-Verlag, Berlin, 1987), and references therein.
[62] L. Gotthard, Solid State Commun. **51**, 975 (1984).
[63] F. Bassani, M. Dressler, and G. Czajkowski, Nuovo Cimento D **20**, 1355 (1998), and references therein.